SPE-176168-MS

Development of Discontinuous Galerkin Methods and a Parallel Simulator for Reservoir Simulation

Kun Wang, University of Calgary; Linbo Zhang, LSEC, Academy of Mathematics and Systems Science, Chinese Academy of Sciences; Zhangxin Chen, University of Calgary

This paper was prepared for presentation at the SPE/IATMI Asia Pacific Oil & Gas Conference and Exhibition held in Nusa Dua, Bali, Indonesia, 20–22 October 2015.

Abstract

The classical discontinuous Galerkin (DG) methods are designed for elliptic (parabolic) problems and hyperbolic problems. For reservoir simulations, the pressure equation from the black oil model is elliptic (parabolic), while the equations for saturations are hyperbolic. Due to this special property, it is difficult to directly apply the discontinuous Galerkin methods to the black oil model. In this paper, we extend the discontinuous Galerkin methods to reservoir simulations. In our schemes, the local discontinuous Galerkin (LDG) method is used to discretize the black oil model. The upwind concept is combined with the numerical flux term of the LDG method to simulate the direction of propagation of the multiphase flow in reservoirs to avoid the unphysical solutions. We also extend the Peaceman model to the discontinuous Galerkin methods on unstructured grids. Based on the extended discontinuous Galerkin methods, we employ the iterative implicit pressure-explicit saturation (iterative-IMPES) and fully implicit (FIM) methods to solve the coupled nonlinear black oil model. A parallel simulator is implemented using the parallel adaptive finite element package, Parallel Hierarchical Grid (PHG), and validated by testing the first and ninth SPE Comparative Solution Projects. The parallel scalability of our simulator is also tested by a large scale case.

Introduction

The discontinuous Galerkin (DG) methods for hyperbolic equations were first introduced by Reed and Hill [22]. Since that time, there has been a lot of research about the DG methods for hyperbolic problems. Cockburn and Shu [7, 8, 9] combined DG discretizations in space and an explicit Runge-Kutta discretization in time and developed the so-called Runge-Kutta discontinuous Galerkin (RKDG) method for nonlinear hyperbolic systems. The local discontinuous Galerkin (LDG) methods [10] are considered as an extension of the RKDG methods to convection-diffusion problems by Bassi and Rebay. Independent of the development of the DG methods for hyperbolic problems, the discontinuous Galerkin methods for the ellipcit and parabolic problems were proposed, and they are generally called interior penalty methods [2, 3, 11, 26, 23].

The DG methods have several properties, which are attractive for porous medium flow calculation. For example, the DG methods are locally mass conservative; they support local approximations of

high order; they are implementable on unstructured and non-matching grids; they can handle strongly discontinuous coefficients. Many researchers have successfully applied the DG methods to reservoir simulations. In [24], the single phase flow problem is solved by a discontinuous Galerkin method. Based on the Non-symmetric Interior Penalty Galerkin (NIPG) method [23], a fully implicit DG method for two phase incompressible flow was performed in [12]. Adaptivity techniques in space and time for the discontinuous Galerkin methods in reservoir simulation were introduced in [16]. In [13, 4], a sequential and a fully-coupled discontinuous Galerkin methods were designed to approximate two phase incompressible flows with discontinuous capillary pressures.

In this paper, we develop a discontinuous Galerkin method for the black oil model on 3D unstructured grids. Our scheme combines the LDG methods with the concept of upwind, which can avoid the appearance of unphysical solutions. We also modify the Peaceman model for the DG method on unstructured grids. The rest of the paper is organized as follows: The mathematical descriptions of the black oil model are introduced first; next, the DG methods are brifely reviewed and extended to the black oil model problem by introducing new fluxes; then the Peaceman model is modified and applied to our discontinuous Galerkin method; after that, our parallel simulator is shortly introduced and validated by testing the first and ninth SPE comparative projects; the parallel scalability of our simulator is also shown in the numerical experiments section; finally, we draw conclusions.

Black Oil Model

The classical black oil model assumes that the flow in a reservoir has three phases and three components (oil, gas and water). Combining Darcy's law and the mass conservation equations, the black oil model is written as follows [6]:

$$\begin{cases} \frac{\partial}{\partial t}(\frac{\phi s_o}{B_o}) = \nabla\cdot(\frac{\mathbf{K}K_{ro}}{\mu_o B_o}\nabla\Phi_o) + q_o, \\ \frac{\partial}{\partial t}(\frac{\phi s_w}{B_w}) = \nabla\cdot(\frac{\mathbf{K}K_{rw}}{\mu_w B_w}\nabla\Phi_w) + q_w, \\ \frac{\partial(\frac{\phi s_o R_s}{B_o}+\frac{\phi s_g}{B_g})}{\partial t} = \nabla\cdot(\frac{\mathbf{K}K_{ro}R_s}{\mu_o B_o}\nabla\Phi_o) + \nabla\cdot(\frac{\mathbf{K}K_{rg}}{\mu_g B_g}\nabla\Phi_g) + q_g, \\ \Phi_\alpha = p_\alpha + \rho_\alpha \wp z, \quad \alpha = o, w, g \\ s_o + s_w + s_g = 1, \\ p_w = p_o - p_{cow}, \\ p_g = p_o + p_{cog}, \end{cases} \tag{1}$$

where ϕ and $\mathbf{K}$ are porosity and permeability, for phase α ($\alpha = o, w, g$), Φ_α is the phase potential, and s_α, μ_α, p_α, B_α, ρ_α, $K_{r\alpha}$ and q_α are the saturation, viscosity, pressure, format volume factor, density, relative permeability and production rate, respectively. p_{cow} and p_{cog} are the oil-water and oil-gas capillary pressures. R_s is the solution gas-oil rate. $\wp$ is the gravitational constant and z is the reservoir depth. These variables have the following relations:

$$
\begin{aligned}
\phi &= \phi(p_o),\\
K_{ro} &= K_{ro}(s_w, s_g),\\
K_{rw} &= K_{rw}(s_w),\\
K_{rg} &= K_{rg}(s_g),\\
\rho_o &= \rho_o(p_o, p_b),\\
\rho_w &= \rho_w(p_w),\\
\rho_g &= \rho_g(p_g),\\
R_s &= R_s(p_o, p_b),\\
\mu_o &= \mu_o(p_o, p_b),\\
\mu_w &= \mu_w(p_w),\\
\mu_g &= \mu_g(p_g),\\
p_{cow} &= p_{cow}(s_w),\\
p_{cog} &= p_{cog}(s_g),
\end{aligned}
$$

where p_b is the bubble point pressure. With proper boundary and initial conditions, a closed system is given.

Extended Discontinuous Galerkin Methods for Black Oil Model

Galerkin methods for partial differential equations are a class of methods of converting a continuous problem to a discrete problem. By converting an equation to a weak formulation, it can be solved on a finite dimensional space. For finite element methods or other continuous Galerkin methods, a function v_c in the finite dimensional space used to approximate the solution is continuous, which means v_c has the same value at the point A in all the four elements K_i, $i = 1,2,3,4$, Fig 1. However, for the discontinuous Galerkin methods, a function v_d may be discontinuous, which is the main difference compared to the continuous Galerkin methods. In Fig 1, at the point A, v_d may have four different value in the four elements.

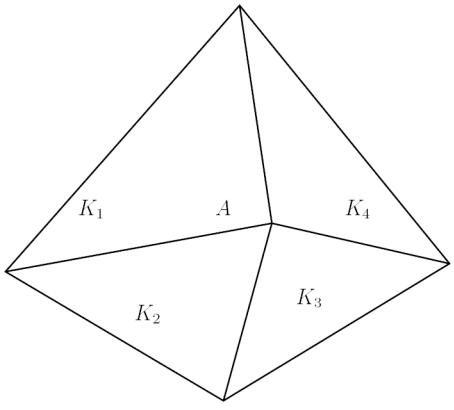

Figure 1—Shared Point

Before introducing the discontinuous Galerkin methods, we first introduce some notation. Let $\Omega_h = \{K_i : i = 1, \ldots, N\}$ be the triangulation of the concerned domain Ω, where N is the total number of elements. We can define the finite element spaces associated with Ω_h by

$$V_h^k := \{v \in L^2(\Omega) : v|_K \in P(K)^k, \forall K \in \Omega_h\}, \tag{2}$$

$$(V_h^k)^3 := \{\tau \in (L^2(\Omega))^3 : \tau|_K \in (P(K)^k)^3, \forall K \in \Omega_h\}, \tag{3}$$

where $P(K)^k$ is the space of polynomial functions of degree at most k on K. Let F be an interior face shared by elements K_1 and K_2, and the unit normal vectors $\vec{n}_1$ and $\vec{n}_2$ on F pointing exterior to K_1 and K_2. For a function $v \in V_h^k$, from the above introduction we know v can have different values on the two sides of the face F, so we define the average $\{v\}$ and the jump $[v]$ on F as

$$\{v\} = \tfrac{1}{2}(v_1 + v_2), \tag{4}$$

$$[v] = v_1\vec{n}_1 + v_2\vec{n}_2, \tag{5}$$

where $v_i := \mathrm{v}|\partial_{Ki}$, $i = 1,2$. For a function $\tau \in (V_h^k)^3$, there are similar definitions of the average $\{\tau\}$ and the jump $[\tau]$ on F as

$$\{\tau\} = \tfrac{1}{2}(\tau_1 + \tau_2), \tag{6}$$

$$[\tau] = \tau_1 \cdot \vec{n}_1 + \tau_2 \cdot \vec{n}_2, \tag{7}$$

where $\tau_i := \mathrm{t}|\partial_{Ki}$, $i = 1,2$. For $e \in \partial\Omega$, we set

$$\{\tau\} = \tau, \tag{8}$$

$$[v] = v\vec{n}, \tag{9}$$

where $\vec{n}$ is the outward unit normal.

With these notation, we take the oil phase equation as an example to illustrate our DG method. The treatment of the water and gas equations is similar. By introducing the auxiliary variable $\vec{u}_o$, which is the oil phase potential difference,

$$\vec{u}_o = \nabla\Phi_o, \tag{10}$$

the mass conservation equation of the oil phase can be written as

$$\frac{\partial}{\partial t}\left(\frac{\phi s_o}{B_o}\right) = \nabla \cdot \left(\frac{\mathbf{K}K_{ro}}{\mu_o B_o}\vec{u}_o\right) + q_o. \tag{11}$$

Multiplying Eqs. (10) and (11) by any test functions $\tau \in (V_h^k)^3$ and $v \in V_h^k$, respectively, and integrating formally on an element K, we get

$$\int_K \vec{u}_o \cdot \tau \mathrm{d}x = -\int_K \Phi_o \nabla \cdot \tau \mathrm{d}x + \int_{\partial K} \Phi_o^* \vec{n} \cdot \tau \mathrm{d}s, \quad \forall \tau \in (V_h^k)^3 \tag{12}$$

$$\int_K \frac{\partial}{\partial t}\left(\frac{\phi s_o}{B_o}\right) v \mathrm{d}x + \int_K K T_o \vec{u}_o \cdot \nabla v \mathrm{d}x = \int_{\partial K} (K T_o \vec{u}_o)^* \cdot \vec{n} v \mathrm{d}s + \int_K q_o v \mathrm{d}x, \quad \forall v \in V_h^k \tag{13}$$

where the oil phase transmissibility $T_o = \frac{K_{ro}}{\mu_o B_o}$, and

$$\begin{cases} \Phi_o^*, \\ (\mathbf{K}T_o\vec{u}_o)^* \end{cases} \tag{14}$$

are numerical fluxes on the boundary of element K. For $\Phi_o \in V_h^k$ and $\mathbf{K}T_o\vec{u}_o \in (V_h^k)^3$, the value on ∂K may be different in element K and in its neighbour elements. Therefore, the numerical fluxes (14) must be defined in terms of Φ_o, $KT_o\vec{u}_o$, and boundary conditions to complete a specific DG method. The choice of the numerical fluxes is quite different from one DG method to another. For the classical LDG method for elliptic problems, the fluxes are chosen as

$$\Phi_o^* = \begin{cases} \{\Phi_o\} - \beta \cdot [\Phi_o] & \text{in} \quad \Omega_h, \\ \Phi_o & \text{on} \quad \partial\Omega_N, \\ \Phi_{o,D} & \text{on} \quad \partial\Omega_D, \end{cases} \tag{15}$$

and

$$(\mathbf{K}T_o\vec{u}_o)^* = \begin{cases} \{\mathbf{K}T_o\vec{u}_o\} + \beta[\mathbf{K}T_o\vec{u}_o] - \gamma[\Phi_o] & \text{in} \quad \Omega_h, \\ \mathbf{K}T_o\vec{u}_o & \text{on} \quad \partial\Omega_D, \\ g_N & \text{on} \quad \partial\Omega_N, \end{cases} \tag{16}$$

where β and γ are penalty parameters[10], Ω_D and Ω_N are the Dirichlet and Neumann boundaries, respectively, and $\Phi_{o,D}$ and g_N are the corresponding boundary conditions.

If the fluxes (15) and (16) are used in Eqs. (12) and (13), unphysical solutions may be obtained due to the hyperbolic property of the black oil model. So we modify the fluxes on the internal faces of $\partial\Omega$ as

$$\Phi_o^* = \{\Phi_o\}, \tag{17}$$

and

$$(\mathbf{K}T_o\vec{u}_o)^* = \overline{\mathbf{K}}\hat{T}_o\{\vec{u}_o\}. \tag{18}$$

In the fluxes (17) and (18), there are three main modifications:

1. The penalty parameters, β and γ, are set to zero, since their effect is negligible in our practical computation.
2. The absolute permeability on the face is approximated by the harmonic average
$$\overline{\mathbf{K}} = \frac{2\mathbf{K}_{T_1}\mathbf{K}_{T_2}}{\mathbf{K}_{T_1} + \mathbf{K}_{T_2}}. \tag{19}$$
The reason for using a harmonic average is that for an inactive element (i.e., the element where $\mathbf{K} = 0$), this average gives the correct value (i.e., $\overline{\mathbf{K}} = 0$), which means that there is no mass transfer between this element and others.
3. The oil phase transmissibility $\hat{T}_o$ is chosen according to the direction of the oil phase flow. In Fig. 2, for the face F shared by elements K_1 and K_2, if the direction of the oil phase flow is from K_1 to K_2, $\hat{T}_o$ is chosen as T_{o,K_1}; if the oil phase flows in the opposite direction, $\hat{T}_o = T_{o,K_2}$. The direction of the flow is decided by the average of the potential difference on the face, $d = \{\vec{u}_o\} \cdot \vec{n}$
$$\hat{T}_o = \begin{cases} T_{o,K_1} & d \le 0, \\ T_{o,K_2} & d > 0. \end{cases} \tag{20}$$

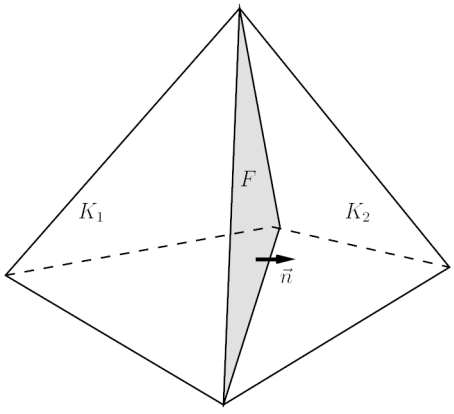

Figure 2—Choice of Transmissibility on Face *F*

Substituting the modified fluxes into Eq. (12) and discretizing the time term by the backward Euler difference scheme, it can be written as

$$\int_K \vec{u}_o^{\,n+1}\cdot\tau \mathrm{d}x = -\int_K \Phi_o^{n+1}\nabla\cdot\tau \mathrm{d}x + \int_{\partial K}\{\Phi_o\}^{n+1}\vec{n}\cdot\tau \mathrm{d}s, \quad \forall\tau\in(V_h^k)^3, \tag{21}$$

$$\int_K \left(\frac{\phi s_o}{B_o}\right)^{n+1} v\mathrm{d}x - \int_K \left(\frac{\phi s_o}{B_o}\right)^{n} v\mathrm{d}x + \int_K \mathbf{K}(T_o\vec{u}_o)^{n+1}\cdot\nabla v\mathrm{d}x = \int_{\partial K}\overline{\mathbf{K}}(\hat{T}_o\{\vec{u}_o\})^{n+1}\cdot\vec{n}v\mathrm{d}s + \int_K q_o^{n+1}v\mathrm{d}x, \quad \forall v\in V_h^k, \tag{22}$$

where $(\cdot)^n$ is the value at the n-th time step, which is already known, and $(\cdot)^{n+1}$ is an unknown value at the next time step. Using Eq. (21), the auxiliary variable $\vec{u}_o$ can be eliminated from Eq. (22). According to different implicity levels, different Newton methods have been developed to solve the above nonlinear equations. The iterative IMPES (implicit pressure and explicit saturation) method and the FIM (fully implicit) method are two of the most popular methods. They have different treatments of the transimissibility term T_o.

For the iterative IMPES method, at the $(l+1)$-th Newton iteration, $T_o^{n+1,l+1}$ is explicitly set to the value at the l-th iteration, which means

$$T_o^{n+1,l+1} = T_o^{n+1,l}. \tag{23}$$

The accumulation term $\left(\frac{\phi s_o}{B_o}\right)^{n+1,l+1}$ treated as

$$\left(\frac{\phi s_o}{B_o}\right)^{n+1,l+1} = \left(\frac{\phi s_o}{B_o}\right)^{n+1,l} + \frac{\partial}{\partial p}\left(\frac{\phi s_o}{B_o}\right)^{n+1,l}\delta p + \frac{\partial}{\partial s_w}\left(\frac{\phi s_o}{B_o}\right)^{n+1,l}\delta s_w + \frac{\partial}{\partial X}\left(\frac{\phi s_o}{B_o}\right)^{n+1,l}\delta X, \tag{24}$$

where $\delta(\cdot)$ is the increment of a primary unknown at the $(l+1)$-th Newton iteration. Substituting Eqs. (23) and (24) into Eq. (22), we have the following stiffness matrix for each element $T\in\Omega_h$,

$$M_{o,p}\vec{\delta p} + M_{o,s_w}\vec{\delta s}_w + M_{o,X}\vec{\delta X} = N_{o,p}\vec{\delta p} + Q_o + \vec{b}_o, \tag{25}$$

where $M_{o,\gamma}$ ($\gamma = p,\ s_w,\ X$) is the matrix resulted from the accumulation term, $N_{o,p}$ is the pressure matrix resulted from the transmissibility term, $\vec{b}_o$ is the right-hand side, and Q_o is from the well term, which will be discussed later. The water phase and gas phase equations have the similar forms as the oil phase equation,

$$M_{w,p}\vec{\delta p} + M_{w,s_w}\vec{\delta s}_w = N_{w,p}\vec{\delta p} + Q_w + \vec{b}_w, \tag{26}$$

$$M_{g,p}\vec{\delta p} + M_{g,s_w}\vec{\delta s}_w + M_{g,X}\vec{\delta X} = N_{g,p}\vec{\delta p} + Q_g + \vec{b}_g. \tag{27}$$

Since the increment of s_w and X appears locally in each element, they can be eliminated by the following Algorithm 1. Consequently, the final linear system is only about the pressure and can be solved efficiently by AMG (algebraic multigrid) methods [25, 19]. After the pressure is solved from the linear system, the saturation and the bubble point pressure can be explicitly calculated using Eqs. (35), (36) and (37).

Algorithm 1—Iterative IMPES Method: eliminate sw and X

1: Multiplying Eq. (36) by $-M_{o,s_w}M_{w,s_w}^{-1}$ and adding the resulting equation to Eq. (35), we get

$$\overline{M_{o,p}}\vec{\delta p}+M_{o,X}\vec{\delta X}=\overline{N_{o,p}}\vec{\delta p}+\overline{Q_o}+\overline{\vec{b}_o}, \tag{28}$$

where

$$\begin{cases}\overline{M_{o,p}}=M_{o,p}-M_{o,s_w}M_{w,s_w}^{-1}M_{w,p},\\ \overline{N_{o,p}}=N_{o,p}-M_{o,s_w}M_{w,s_w}^{-1}N_{w,p},\\ \overline{Q_o}=Q_o-M_{o,s_w}M_{w,s_w}^{-1}Q_w,\\ \overline{\vec{b}_o}=\vec{b}_o-M_{o,s_w}M_{w,s_w}^{-1}\vec{b}_w.\end{cases} \tag{29}$$

2: Multiplying Eq. (36) by $-M_{g,s_w}M_{w,s_w}^{-1}$ and adding the resulting equation to Eq. (37), we get

$$\overline{M_{g,p}}\vec{\delta p}+M_{g,X}\vec{\delta X}=\overline{N_{g,p}}\vec{\delta p}+\overline{Q_g}+\overline{\vec{b}_g}, \tag{30}$$

where

$$\begin{cases}\overline{M_{g,p}}=M_{g,p}-M_{g,s_w}M_{w,s_w}^{-1}M_{w,p},\\ \overline{N_{g,p}}=N_{g,p}-M_{g,s_w}M_{w,s_w}^{-1}N_{w,p},\\ \overline{Q_g}=Q_g-M_{g,s_w}M_{w,s_w}^{-1}Q_w,\\ \overline{\vec{b}_g}=\vec{b}_g-M_{g,s_w}M_{w,s_w}^{-1}\vec{b}_w.\end{cases} \tag{31}$$

3: Multiplying Eq. (30) by $-M_{o,X}M_{g,X}^{-1}$ and adding the resulting equation to Eq. (28), we get

$$\hat{M_{o,p}}\vec{\delta p}=\hat{N_{o,p}}\vec{\delta p}+\hat{Q_o}+\hat{\vec{b}_o}, \tag{32}$$

where

$$\begin{cases}\hat{M_{o,p}}=\overline{M_{o,p}}-M_{o,X}M_{g,X}^{-1}\overline{M_{g,p}},\\ \hat{N_{o,p}}=\overline{N_{o,p}}-M_{o,X}M_{g,X}^{-1}\overline{N_{g,p}},\\ \hat{Q_o}=\overline{Q_o}-M_{o,X}M_{g,X}^{-1}\overline{Q_g},\\ \hat{\vec{b}_o}=\overline{\vec{b}_o}-M_{o,X}M_{g,X}^{-1}\overline{\vec{b}_g}.\end{cases} \tag{33}$$

For the FIM method, $T_o^{n+1,l+1}$ is handled implicitly as

$$T_o^{n+1,l+1}=T_o^{n+1,l}+\left(\frac{\partial T_o}{\partial p}\right)^{n+1,l}\delta p+\left(\frac{\partial T_o}{\partial s_w}\right)^{n+1,l}\delta s_w+\left(\frac{\partial T_o}{\partial X}\right)^{n+1,l}\delta X. \tag{34}$$

The treatment of the accumulation term in the FIM method is the same as in the iterative IMPES method. Substituting Eqs. (34) and (24) into Eq. (22), we get

$$M_{o,p}\vec{\delta p}+M_{o,s_w}\vec{\delta s}_w+M_{o,X}\vec{\delta X}=N_{o,p}\vec{\delta p}+N_{o,s_w}\vec{\delta s}_w+N_{o,X}\vec{\delta X}+Q_o+\vec{b}_o, \tag{35}$$

$$M_{w,p}\vec{\delta p}+M_{w,s_w}\vec{\delta s}_w=N_{w,p}\vec{\delta p}+N_{w,s_w}\vec{\delta s}_w+Q_w+\vec{b}_w, \tag{36}$$

$$M_{g,p}\vec{\delta p}+M_{g,s_w}\vec{\delta s}_w+M_{g,X}\vec{\delta X}=N_{g,p}\vec{\delta p}+N_{g,s_w}\vec{\delta s}_w+N_{g,X}\vec{\delta X}+Q_g+\vec{b}_g, \tag{37}$$

where N_γ ($\gamma = s_w, X$) is the matrix corresponding to the increment of s_w and X resulted from the transmissibility term. Because of N_γ ($\gamma = s_w, X$), the three primary unknowns must be solved simultaneously, which creates diffculties for the solution of the linear system. Efficient preconditioners, such as constrained pressure residual (CPR) [27, 5, 17], multistage [1] and fast auxiliary space preconditioners (FASP) [14], have been developed to solve the linear systems resulted from the FIM method.

Treatment of Wells

For the well term in Eq. (22), the first comprehensive model was introduced by Peaceman [21], which is developed for cell-centered finite difference methods on square grids. So far, the Peaceman model and its extensions are still the most widely used methods to model the well flow rate constraints. We first introduce the derivation of the Peaceman model, and then modify it for the discontinuous Galerkin method on the unstructured grids. Assume the flow near a well is steady, and the Darcy law for a single phase problem at the radial direction is

$$q = \frac{-2\pi K_H h_W r_W}{\mu} \frac{\partial p}{\partial t}\Big|_{r=r_W}, \tag{38}$$

where K_h is the horizontal absolute permeability ($K_H = \sqrt{K_x K_y}$, where K_x and K_y are the absolute permeability in directions x and y, respectively), h_w is the height of the well, and r_w is the radius of the wellbore. Separating variables and integrating both sides of Eq. (38) through the region [rw, r], we have

$$\int_{r_w}^{r} \frac{1}{r}\partial r = \frac{-2\pi K_H h_W}{q\mu} \int_{p_{wf}}^{p} \partial p, \tag{39}$$

where p_{wp} is the pressure at the wellbore (also called a bottom-hole pressure). Consequently, we obtain

$$p = p_{Wf} - \frac{q\mu}{2\pi K_H h_W} \ln\left(\frac{r}{r_W}\right). \tag{40}$$

Let $\overline{p}$ be the average of p in the region [r_w,r],

$$\overline{p} = \frac{\int_{r_w}^{r} 2\pi r h_W p \mathrm{d}r}{\int_{r_w}^{r} 2\pi r h_W \mathrm{d}r} \tag{41}$$

Substituting Eq. (40) into Eq. (41), we obtain

$$\begin{aligned} \overline{p} &= \frac{2}{r^2 - r_W^2} \int_{r_w}^{r} \left[p_{Wf} - \frac{q\mu}{2\pi K_H h_W} \ln\left(\frac{r}{r_W}\right) \right] r \mathrm{d}r \\ &= p_{Wf} - \frac{q\mu}{2\pi K_H h_W (r^2 - r_W^2)} \left[r^2 \ln\left(\frac{r}{r_W}\right) - \frac{1}{2}(r^2 - r_W^2) \right]. \end{aligned}$$

When $r \gg r_w$, the above formula can be simplified as

$$\overline{p} = p_{Wf} - \frac{q\mu}{2\pi K_H h_W} \left[\ln\left(\frac{r}{r_W}\right) - \frac{1}{2} \right]. \tag{42}$$

At the surface condition, the formation volume factor B should be added to Eq. (42), and Eq. (42) becomes

$$\overline{p} = p_{Wf} - \frac{q_s \mu B}{2\pi K_H h_W} \left[\ln\left(\frac{r}{r_W}\right) - \frac{1}{2} \right], \tag{43}$$

where q_s is the flow rate at the surface condition. On a cube grid, the radius r is replaced by an equivalent radius r_e,

$$r_e = 0.28 \frac{\{[(K_y/K_x)^{1/2}(\Delta x)^2] + [(K_x/K_y)^{1/2}(\Delta y)^2]\}^{1/2}}{(K_y/K_x)^{1/4} + (K_x/K_y)^{1/4}}, \tag{44}$$

where Δx, Δy and Δz are the dimensions of the cube in the x, y and z directions, respectively.

When we use the discontinuous Galerkin method on unstructured grids, we first partition the region near the well into hexahedrons, and then repartition the hexahedrons into tetrahedrons; see Fig 3. Integrating Eq. (40) on the well region Ω_w and employing the equivalent radius r_e of the Peaceman model, we obtain

$$
\begin{aligned}
q_s &= \frac{1}{\mathrm{vol}(\Omega_w)} \int_{\Omega_w} \frac{-2\pi K_H h_w}{\mu B \ln(r_e/r_w)} (p_e - p_{wf}) \mathrm{d}x \\
&= \frac{1}{\mathrm{vol}(\Omega_w)} \int_{\Omega_w} \frac{-2\pi h_w}{\ln(r_e/r_w)} \frac{K_H}{\mu B} (p - p_{wf}) \mathrm{d}x \\
&= \frac{1}{\mathrm{vol}(\Omega_w)} \sum_{T \in \Omega_w} \int_T \frac{-2\pi h_w}{\ln(r_e/r_w)} \frac{K_H}{\mu B} (p - p_{wf}) \mathrm{d}x,
\end{aligned} \tag{45}
$$

where $\mathrm{vol}(\Omega_w)$ is the total volume of Ω_w. Finally, we get the modified Peaceman model (45) for the discontinuous Galerkin methods on unstructured grids.

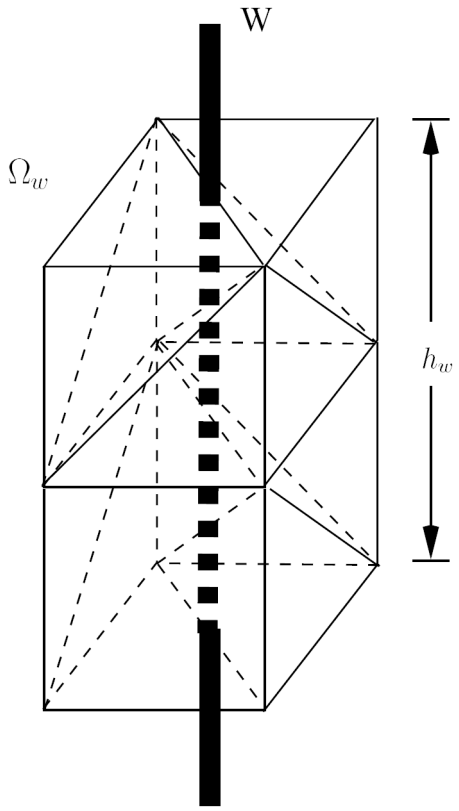

Figure 3—Partition of the Well Region

A Parallel Simulator

PHG (Parallel Hierarchical Grid) [28, 29,18] is a toolbox for developing parallel adaptive finite element programs. PHG is currently under active development at State Key Laboratory of Scientific and Engineering Computing of Chinese Academy of Sciences. PHG deals with conforming tetrahedral meshes. For parallel processing, PHG uses MPI for message passing. It partitions a mesh into submeshes and distributes the submeshes onto individual MPI processors. PHG supports fully parallel local mesh refinement and coarsening based on a tetrahedron bisection algorithm.

Based on PHG, we implemented a parallel black oil simulator using the extended discontinuous Galerkin methods. Benifiting from the powerful software PHG, our parallel black oil simulator has the ability of efficiently handling large scale reservoir simulations, parallel mesh adaptation, using arbitrary high order base functions, and calling linear solver packages, including PETSc, Hypre, SuperLU, MUMPS and Trilinos, by the supplied interfaces. Using tetrahedron elements, our simulator can easily deal with complex geology features, including faults, channels and pinchouts. With the local mesh

refinement and coarsening techniques, more grids can be put on the concerned regions, and non-essential grids can be eliminated, which makes the computation more efficient.

Numerical Experiments

SPE1 Case

First, we use the SPE benchmark problem of Odeh for gas injection to validate our simulator. This is a standard three-phase black oil model, with $10 \times 10 \times 3$ cubic grid blocks and isotropic and layered permeability. One high rate gas injector and one producer are located at two opposite corners. The total simulation time is 10 years. Details of this case can be found in [20].

In our simulation, we divide each cubic block into six tetrahedrons. The simulation results are compared between our simulator and Eclipse by Schlumberger. The oil production rate, the gas/oil production rate (GOR) and the bottom hole pressure of the producer are shown in Figs. 5, 6 and 7, from which we can see that the results match well.

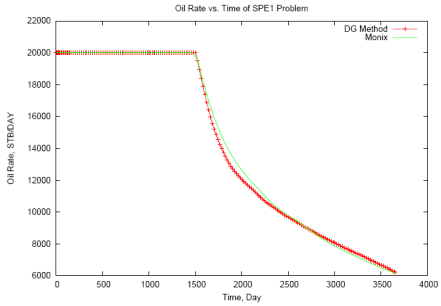

Figure 5—SPE1 case: Oil Rate vs. Time

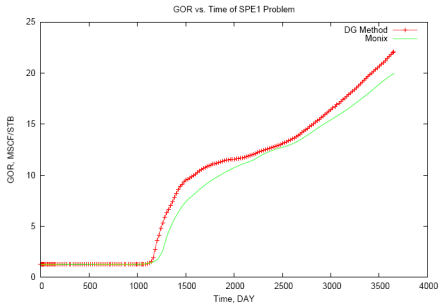

Figure 6—SPE1 case: GOR vs. time

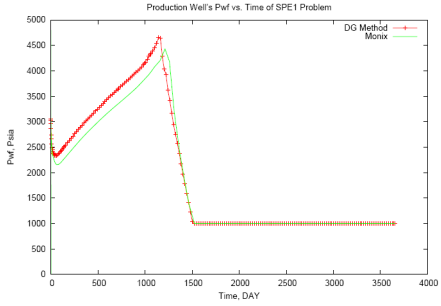

Figure 7—SPE1 case: Production Well Bottom Hole Pressure vs. time

SPE9 Case

The Ninth Comparative Solution Project, which is based on a 24 × 25 × 15 grid placed on a dipping reservoir, is designed to reexamine 3D black oil simulators. The SPE9 reservoir model uses a highly hetergenous geostatistically based permeability field. The model contains one water injection well and 25 production wells. More details can be found in [15].

In this simulation, hexahedrons are also divided into tetrahedrons the same way as in the SPE1 case. The initial pressure and water saturation are calculated by hydrostatic equations and shown in Figs. 8 and 9. We randomly selected four producers and compared the bottom hole pressure with Eclipse. The results are shown in Figs 10–13. The gas saturation of the field at specific times is shown in Figs. 14–19.

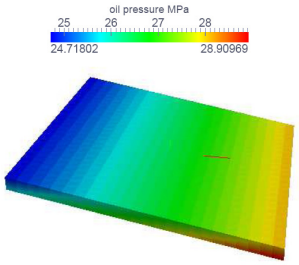

Figure 8—SPE9: Initial Pressure

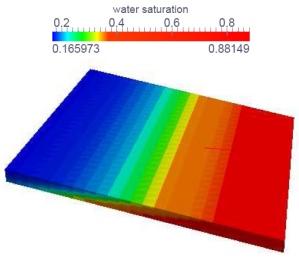

Figure 9—SPE9: Initial Water Saturation

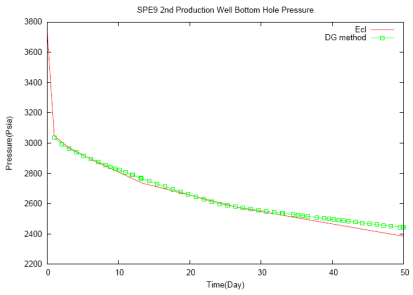

Figure 10—SPE9: 2nd Producer

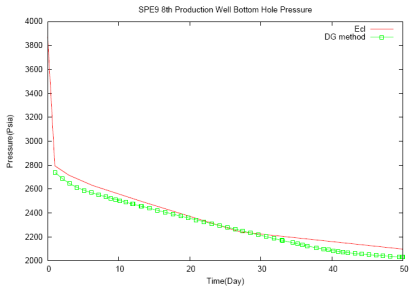

Figure 11—SPE9: 8th Producer

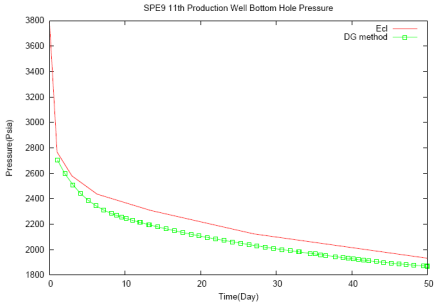

Figure 12—SPE9: 11th Producer

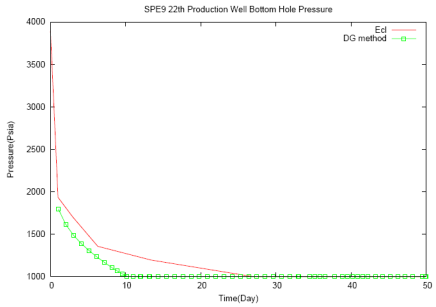

Figure 13—SPE9: 22th Producer

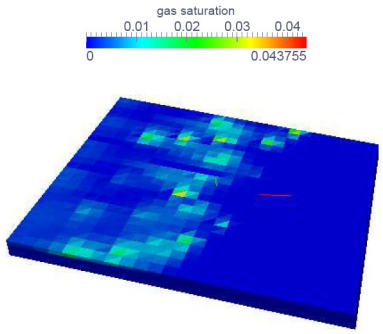

Figure 14—6.15 Day

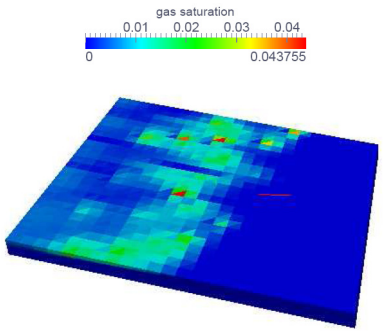

Figure 15—11.29 Day

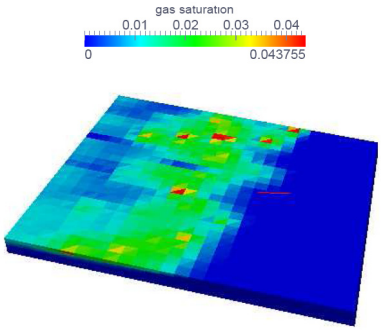

Figure 16—22.68 Day

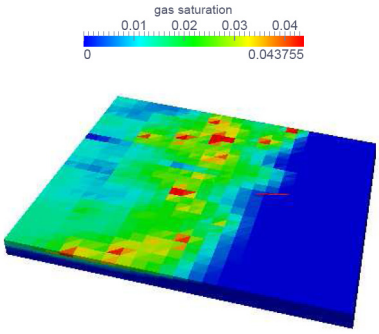

Figure 17—33.70 Day

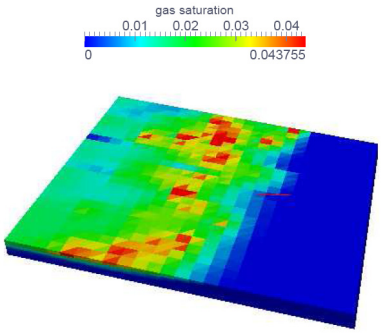

Figure 18—41.84 Day

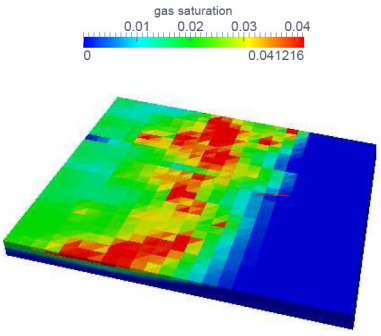

Figure 19—50 Day

Oil-Water Two Phase Case

This is an oil-water two phase case. We use this case to test the parallel scalability of our simulator. It is tested on the cluster LSSC-III of the State Key Laboratory of Scientfic and Engineering Computing of

China, which consists of 282 computing nodes with dual Intel Xeon X5550 quad-core CPUs, interconnected via DDR InfiniBand network. In this case, the relative permeability is calculated by

$$K_{ro} = (K_{ro})_{S_{wc}} \left(\frac{1 - s_w - s_{orw}}{1 - s_{wc} - s_{orw}} \right)^{n_o} \tag{46}$$

$$K_{rw} = (K_{rw})_{S_{orw}} \left(\frac{s_w - s_{wc}}{1 - s_{wc} - s_{orw}} \right)^{n_w} \tag{47}$$

The detailed description of this case is as follows:

- Reservoir region: $\Omega = [0,400\text{m}] \times [0,400\text{m}] \times [0,10\text{m}]$.
- Initial condition: $p = 20\text{MPa}$, $s_o = 0.6$, and $s_w = 0.4$.
- Well is located at the center of the field. The oil production rate is fixed at $10\text{m}^3/\text{day}$.
- Rock and fluid properties:
  - Absolute permeability: $K_x = K_y = Kz = 100\text{mD}$.
  - Porosity: $\phi = 0.2$ at $p = 20\text{MPa}$, rock compressibility $c_\phi = 0.00015\text{MPa}^{-1}$.
  - Relative permeability: $S_{orw} = 0$, $(K_{rw})s_{orw} = 0.6$, $(K_m)s_w c = 1$, $Swc = 0$, $no = 4$, and $n_w = 3$.
  - Oil property: $B_o = 1.05$, compressibility $c_o = 0.002\text{MPa}^{-1}$, $\mu_o = 1\text{mPa·s}$.
  - Water property: $B_w = 1.02$, compressibility $c_w = 0.001\text{MPa}^{-1}$, $\mu_w = 0.1\text{mPa·s}$.
- Total simulation time: 30 days.

In Tables 1 and 2, ″Avg. Newton″ is the average number of Newton iterations for each time step, and ″Avg. Linear″ is the average number of linear iterations for each Newton iteration. In order to test the weak parallel scalability, we fix the number of DOFs (degrees of freedom) on each process, and use 2 to 128 processors. The weak parallel scalability is shown in Table 1. For the strong scalability test, we fix the number of total DOFs (5,164,032), and use 32 to 256 processors. The strong scalability is shown in Table 2.

Table 1—Weak Scalability

processes	DOFs	Avg. Newton	Avg. Linear	Time Cost	Scalability
2	10584	4.0	18.3	4.50 secs	-
16	84672	4.0	21.3	4.54 secs	0.99
64	338688	4.0	27.5	6.83 secs	0.66
128	677376	4.0	35.6	9.76 secs	0.46

Table 2—Strong Scalability

processes	Avg. Newton	Avg. Linear	Time Cost	Scalability
32	4.2	66.5	219.4 secs	-
64	4.2	67.4	128.3 secs	0.85
128	4.2	68.8	61.2 secs	0.90
256	4.2	69.0	36.5 secs	0.85

Conclusions

In this paper, the extended discontinuous Galerkin method for the black oil model problem has been developed. The numerical fluxes of the classical LDG method are modified by removing the penalty

terms, using a harmonic average permeability and adding the upwind concept. The new fluxes can avoid the unphysical solutions during simulation. The extended discontinuous Galerkin method can be directly applied to other kinds of reservoir simulations, such as compositional and thermal simulations. The Peaceman well model on unstructured grids is also developed. With our schemes, we have implemented a parallel black oil simulator using the parallel adaptive finite element toolbox PHG. In the numerical experiment section, our simulator is validated by comparing the results of SPE1 and SPE9 with Eclipse. To test the parallel scalability of our simulator, a large scale oil-water two phase problem is performed. Good weak scalability and strong scalability are obtained in this case.

Acknowledgements

The support of Department of Chemical and Petroleum Engineering, University of Calgary, Reservoir Simulation Group and Academy of Mathematics and Systems Science, Chinese Academy of Sciences, is gratefully acknowledged. The research is also partly supported by NSERC/AIEES/Foundation CMG and AITF Chairs, as well as by National 973 Project of China (2011CB309703), National 863 Project of China (2012AA01A309), China NSF (91430215,11321061), and National Center for Mathematics and Interdisciplinary Sciences of Chinese Academy of Sciences.

References

1. T. M. Al-Shaalan, H. M. Klie, A. H. Dogru, M. F. Wheeler, Studies of robust two stage preconditioners for the solution of fully implicit multiphase flow problems, in: *SPE Reservoir Simulation Symposium,* 2009.
2. D. N. Arnold, An interior penalty finite element method with discontinuous elements, *SIAM J. Numer. Anal*., **19** (1982), pp. 742760.
3. G. A. Baker, Finite element methods for elliptic equations using nonconforming elements, *Math. Comp*., **31** (1977), pp. 4559.
4. P. Bastian, A fully-coupled discontinuous Galerkin method for two-phase flow in porous media with discontinuous capillary pressure. *Computational Geosciences* **18.5** (2014): 779–796.
5. H. Cao, H. A. Tchelepi, J. R. Wallis, H. E. Yardumian, Parallel scalable unstructured cpr-type linear solver for reservoir simulation, in: *SPE Annual Technical Conference and Exhibition,* 2005.
6. Z. Chen, G. Huan, and Y. Ma. *Computational methods for multiphase flows in porous media*. Vol. **2**. Siam, 2006.
7. B. Cockburn, C.-W. Shu, TVB Runge-Kutta local projection discontinuous Galerkin finite element method for conservation laws ii: General framework. *Math. Comput*., **52**(1989), 411–435.
8. B. Cockburn, S. Hou, C.-W. Shu, TVB Runge-Kutta local projection discontinuous Galerkin finite element method for conservation laws iii: One dimensional systems. *J. Comput. Phys*., **84**(1989), 90–113.
9. B. Cockburn, C.-W. Shu, TVB Runge-Kutta local projection discontinuous Galerkin finite element method for conservation laws iv: The multidimensional case. *Math. Comput*., **54**(1990), 545i–581.
10. B. Cockburn, C.-W. Shu, The local discontinuous Galerkin method for time-dependent convection-diffusion systems. *J. Numer. Anal*., **35**(1998), 2440–2463.
11. J. Douglas, Jr. and T. Dupont, Interior Penalty Procedures for Elliptic and Parabolic Galerkin Methods, *Lecture Notes in Phys*. **58,** Springer-Verlag, Berlin, 1976.
12. Y. Epshteyn and B. Riviere. Fully Implicit Discontinuous Finite Element Methods for Two- Phase Flow, *Applied Numerical Mathematics,* **57**(2007), 383–401.
13. A. Ern, I. Mozolevski, and L. Schuh. Discontinuous Galerkin approximation of two-phase flows in heterogeneous porous media with discontinuous capillary pressures. *Computer methods in applied mechanics and engineering* **199.23** (2010): 1491–1501.

14. X. Hu, W. Liu, G. Qin, J. Xu, C. Zhang, Development of a fast auxiliary subspace pre-conditioner for numerical reservoir simulators, in: SPE Reservoir Characterisation and Simulation Conference and Exhibition, 2011.
15. J. E. Killough, Ninth SPE comparative solution project: a reexamination of black-oil simulation, SPE Reservoir Simulation Symposium. Society of Petroleum Engineers, 1995.
16. W. Klieber, B. Riviere, Adaptive simulations of two-phase flow by discontinuous Galerkin methods, *Computer Methods in Applied Mechanics and Engineering,* **196**(2006), 404–419.
17. H. Liu, K. Wang, Z. Chen, K. E. Jordan, Efficient multi-stage preconditioners for highly heterogeneous reservoir simulations on parallel distributed systems, in: SPE Reservoir Simulation Symposium. Society of Petroleum Engineers, 2015.
18. H. Liu, Z. Chen and L.B. Zhang, Parallel construction of Hamiltonian paths for conforming tetrahedral Meshes, *International Journal of Computer Mathematics,* **90**(7): 1366–1372, 2013.
19. H. Liu, S. Yu and Z. Chen, Development of algebraic multigrid solvers using GPUs, SPE-163661-MS, SPE Reservoir Simulation Symposium, Houston, USA, Feb 2013.
20. A. Odeh, Comparison of solutions to a three-dimensional black-oil reservoir simulation problem (includes associated paper 9741), *Journal of Petroleum Technology* **33.1** (1981): 13–25.
21. D. W. Peaceman, Interpretation of well-block pressures in numerical reservoir simulation, SPE 6893, The 52nd Annual Fall Technical Conference and Exhibition, Denver, CO.
22. W.H. Reed and T.R. Hill, Triangular mesh method for the neutron transport equation, Technical report LA-UR-73–479, Los Alamos Scientific Laboratory, Los. Alamos, NM, 1973.
23. B. Riviere, M. F. Wheeler, and V. Girault, Improved energy estimates for interior penalty, constrained and discontinuous Galerkin methods for elliptic problems I, Comput. *Geosci*., **3** (1999), pp. 337360.
24. B. Riviere, M. F. Wheeler and K. Banas, Part ii. Discontinuous Galerkin method applied to a single phase flow in porous media. *Coumput. Geosci*., **4**(2000), 337–349.
25. K. Stüben, *Algebraic multigrid (amg): an introduction with applications, in: GMD-Forschungszentrum Informationstechnik,* 1999.
26. M. F. Wheeler, An elliptic collocation-finite element method with interior penalties, *SIAM J. Numer. Anal*., **15** (1978), pp. 152161.
27. J. R. Wallis, R. P. Kendall, T. E. Little, Constrained residual acceleration of conjugate residual methods, in: SPE Reservoir Simulation Symposium, 1985.
28. L.B. Zhang, *Parallel Hierarchical Grid,* http://lsec.cc.ac.cn/phg/index_en.htm/.
29. L.B. Zhang, T. Cui and H. Liu, A set of symmetric quadrature rules on triangles and tetrahedra, *J.Comp.Math,* **27** (1): 89–96, 2009.